higher titer vector, whereas the three births, including the transgenic one, and the blighted pregnancy originated from the lower titer LNEFEGFP-(VSV-G) vector (10^8 cfu/ml; Table 1). Although only one live offspring is shown to be transgenic, we cannot yet exclude the possibility of transgenic mosaics in the others. We have neither demonstrated germline transmission nor the presence of transgenic sperm; this must await ANDi's development through puberty in about 4 years. Vector titers and volume injected may play crucial roles in gene transfer efficiency. These offspring and their surrogates are now housed in dedicated facilities with ongoing, stringent monitoring.

Nonhuman primates are invaluable models for advancing gene therapy treatments for diseases such as Parkinson's (*24*) and diabetes (*25*), as well as ideal models for testing cell therapies (*26*) and vaccines, including those for HIV (*27, 28*). Although we have demonstrated transgene introduction in rhesus monkeys, significant hurdles remain for the successful homologous recombination essential for gene targeting (*29*). The molecular approaches for making clones [either by embryo splitting (*30*) or nuclear transfer (*31–36*)], utilizing stem cells (*37–39*), and now producing transgenic monkeys, could be combined to produce the ideal models to accelerate discoveries and to bridge the scientific gap between transgenic mice and humans.

References and Notes

1. M. J. Blouin *et al.*, *Nature Med.* **6**, 177 (2000).
2. R. L. Eckert *et al.*, *Int. J. Oncol.* **16**, 853 (2000).
3. H. M. Hsieh-Li *et al.*, *Nature Genet.* **24**, 66 (2000).
4. A. M. Murphy *et al.*, *Science* **287**, 488 (2000).
5. E. J. Weinstein *et al.*, *Mol. Med.* **6**, 4 (2000).
6. J. A. Thomson, V. S. Marshall, *Curr. Topics Dev. Biol.* **38**, 133 (1998).
7. A. W. S. Chan *et al.*, *Mol. Hum. Reprod.* **6**, 26 (2000).
8. K. R. Chien, *J. Clin. Invest.* **98**, S19 (1996).
9. R. P. Erickson, *BioEssays* **18**, 993 (1996).
10. A. W. S. Chan *et al.*, *Proc. Natl. Acad. Sci. U.S.A.* **95**, 14028 (1998).
11. J. K. Yee *et al.*, *Methods Cell Biol.* **43**, 99 (1994).
12. The GFP vector was injected into the perivitelline space (*10*) of in vivo matured rhesus oocytes (*40*), fertilized by ICSI 6 hours later. Embryos at the four- to eight-cell stage were selected for embryo transfer on the basis of morphology. Surrogate females were selected on the basis of serum estradiol and progesterone levels (*15*).
13. The GFP gene from plasmid pEGFP-N1 was inserted into the retroviral vector pLNCX using standard recombinant DNA techniques [Web supplement 1 (*41*)].
14. Oocytes for electron microscopy were fixed in Ito-Karnovsky's fixative [Web supplement 2 (*41*)].
15. L. Hewitson *et al.*, *Hum. Reprod.* **13**, 2786 (1998).
16. L. Hewitson *et al.*, *Nature Med.* **5**, 431 (1999).
17. Genomic DNA was extracted from tissues obtained from the stillbirths [Web supplement 3 (*41*)].
18. PCR was performed using specific primers that amplify the flanking region of the GFP gene. Provirus was detected by using a primer set specific to the unique LTR region of genomic integrated virus. Transgene was detected by standard reverse transcription followed by PCR [Web supplement 4 (*41*)].
19. Southern analysis was performed using genomic DNA followed by restriction enzyme digestion using a unique site within the vector and detected by a GFP [^{32}P]-labeled probe [Web supplement 5 (*41*)].
20. B. Schott *et al.*, *Nucleic Acid Res.* **25**, 2940 (1997).
21. N. Chinnasamy *et al.*, *Hum. Gene Ther.* **11**, 1901 (2000).
22. Biopsied tissues were snap frozen, sectioned, fixed, and imaged with anti-GFP using rhodamine-conjugated anti-mouse (IgG) secondary antibody [Web supplement 6 (*41*)].
23. T. Roe *et al.*, *EMBO J.* **12**, 2099 (1993).
24. J. H. Kordower *et al.*, *Science* **290**, 767 (2000).
25. H. C. Lee *et al.*, *Nature* **408**, 483 (2000).
26. D. H. Barouch *et al.*, *Proc. Natl. Acad. Sci. U.S.A.* **97**, 4192 (2000).
27. M. J. Kuroda *et al.*, *J. Virol.* **74**, 8751 (2000).
28. N. Nathanson *et al.*, *AIDS (suppl. A)* **13**, S113 (1999).
29. U. Muller, *Mech. Dev.* **82**, 1 (1999).
30. A. W. S. Chan *et al.*, *Science* **287**, 317 (2000).
31. I. Wilmut *et al.*, *Nature* **385**, 810 (1997).
32. J. B. Cibelli *et al.*, *Science* **280**, 1256 (1998).
33. T. Wakayama *et al.*, *Nature* **394**, 369 (1998).
34. D. P. Wolf *et al.*, *Biol. Reprod.* **60**, 199 (1999).
35. A. Onishi *et al.*, *Science* **289**, 1188 (2000).
36. I. A. Polejaeva *et al.*, *Nature* **407**, 86 (2000).
37. J. A. Thomson *et al.*, *Proc. Natl. Acad. Sci. U.S.A.* **92**, 7844 (1995).
38. M. J. Shamblott *et al.*, *Proc. Natl. Acad. Sci. U.S.A.* **95**, 13726 (1998).
39. J. A. Thomson *et al.*, *Science* **282**, 1145 (1998).
40. G. J. Wu *et al.*, *Biol. Reprod.* **55**, 269 (1996).
41. Supplementary figures are available at www.sciencemag.org/cgi/content/full/291/5502/309/DC1.
42. A. W. S. Chan, K. Y. Chong, C. Martinovich, C. Simerly, G. Schatten, data not shown.

43. We thank J. C. Burns (University of California San Diego); B. True (University of Wisconsin–Madison); K. Wells (U.S. Department of Agriculture); Chiron Inc.; and all at the Oregon Regional Primate Research Center (ORPRC), especially M. Axthelm, J. Bassir, J. M. Cook, N. Duncan, M. Emme, J. Fanton, A. Hall, L. Hewitson, D. Jacob, E. Jacoby, A. Lewis, C. M. Luetjens, C. Machida, G. Macginnis, B. Mason, T. Swanson, D. Takahashi, K. Tice, J. Vidgoff, M. Webb, and S. Wong. Procedures approved by the Oregon Health Sciences University/ORPRC Animal Care and Biosafety Committees. Supported by NIH/National Center for Research Resources (NCRR) (ORPRC; M. S. Smith, Director) and grants (NCRR, National Institute of Child Health and Human Development to G.S.).

7 November 2000; accepted 14 December 2000

Categorical Representation of Visual Stimuli in the Primate Prefrontal Cortex

David J. Freedman,[1,2,5] Maximilian Riesenhuber,[3,4,5] Tomaso Poggio,[3,4,5] Earl K. Miller[1,2,5]*

The ability to group stimuli into meaningful categories is a fundamental cognitive process. To explore its neural basis, we trained monkeys to categorize computer-generated stimuli as "cats" and "dogs." A morphing system was used to systematically vary stimulus shape and precisely define the category boundary. Neural activity in the lateral prefrontal cortex reflected the category of visual stimuli, even when a monkey was retrained with the stimuli assigned to new categories.

Categorization refers to the ability to react similarly to stimuli when they are physically distinct, and to react differently to stimuli that may be physically similar (*1*). For example, we recognize an apple and a banana to be in the same category (food) even though they are dissimilar in appearance, and we consider an apple and a billiard ball to be in different categories even though they are similar in shape and sometimes color. Categorization is fundamental; our raw perceptions would be useless without our classification of items as furniture or food. Although a great deal is known about the neural analysis of visual features, little is known about the neural basis of the categorical information that gives them meaning.

In advanced animals, most categories are learned. Monkeys can learn to categorize stimuli as animal or non-animal (*2*), food or non-food (*3*), tree or non-tree, fish or non-fish (*4*), and by ordinal number (*5*). The neural correlate of such perceptual categories might be found in brain areas that process visual form. The inferior temporal (IT) and prefrontal (PF) cortices are likely candidates; their neurons are sensitive to form (*6–9*) and they are important for a wide range of visual behaviors (*10–12*).

The hallmark of perceptual categorization is a sharp "boundary" (*13*). That is, stimuli from different categories that are similar in appearance (e.g., apple/billiard ball) are treated as different, whereas distinct stimuli within the same category (e.g., apple/banana) are treated alike. Presumably, there are neurons that also represent such sharp distinctions. This is difficult to assess with a small subset of a large, amorphous category (e.g., food, human, etc). Because the category boundary is unknown, it is unclear whether neural activity reflects category membership or physical similarity.

[1]Center for Learning and Memory, [2]RIKEN-MIT Neuroscience Research Center, [3]Center for Biological and Computational Learning, [4]McGovern Institute for Brain Research, [5]Department of Brain and Cognitive Sciences, Massachusetts Institute of Technology, Cambridge, MA 02139, USA.

*To whom correspondence should be addressed. E-mail: ekm@ai.mit.edu

We used a three-dimensional morphing system to generate stimuli that spanned two categories, "cats" and "dogs." Three species of cats and three breeds of dogs served as prototypes (*14*–*16*); the morphed images were linear combinations of all possible arrangements between them (Fig. 1). By blending different amounts of "cat" and "dog," we could continuously vary the shape and precisely define the category boundary (*17*). Thus, stimuli that were close to but on opposite sides of the boundary could be similar, whereas stimuli that belonged to the same category could be dissimilar (e.g., "cheetah" and "housecat") (*18*).

Two monkeys performed a delayed match-to-category (DMC) task (Fig. 2A) that required judging whether a sample and test stimulus were from the same category (*19*). Performance was high (about 90% correct), even when the samples were close to the category boundary (Fig. 2B). The monkeys classified dog-like cats (60:40 cat:dog) correctly about 90% of the time, and misclassified them as dogs only 10% of the time; they did as well with cat-like dogs (60:40 dog:cat).

We made recordings from 395 neurons from the lateral PF cortices of two monkeys (*20*) (Fig. 3A). The majority of neurons were activated during the sample and/or delay interval (253/395 or 64%) (*21*). They often reflected the sample's category. Nearly one-third of responsive neurons (82/253) were category-selective in that they exhibited an overall difference

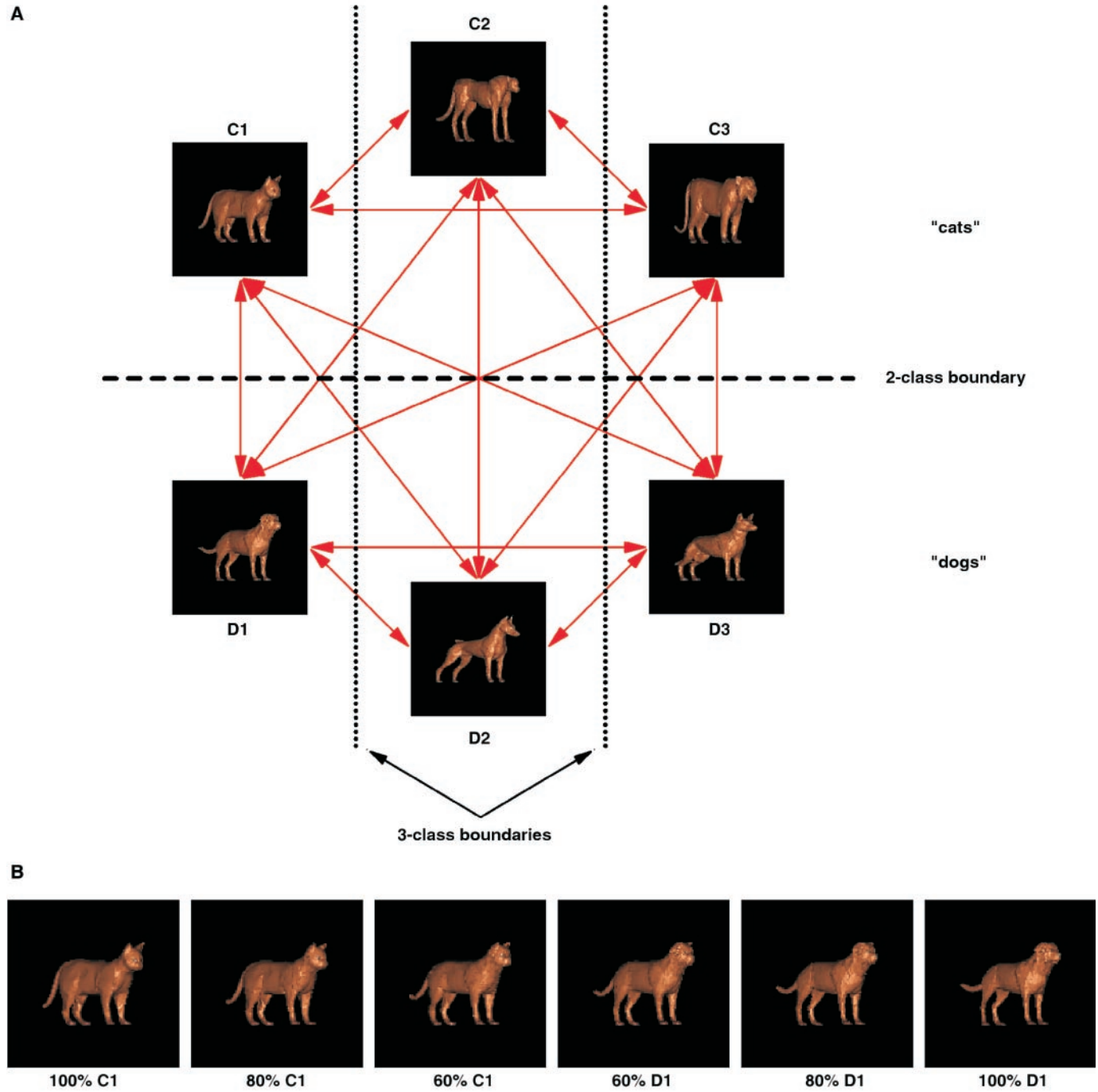

Fig. 1. The stimuli. (**A**) Monkeys learned to categorize randomly generated "morphs" from the vast number of possible blends of six prototypes. For neurophysiological recording, 54 sample stimuli were constructed along the 15 morph lines illustrated here. The placement of the prototypes in this diagram does not reflect their similarity. (**B**) Morphs along the C1-D1 line.

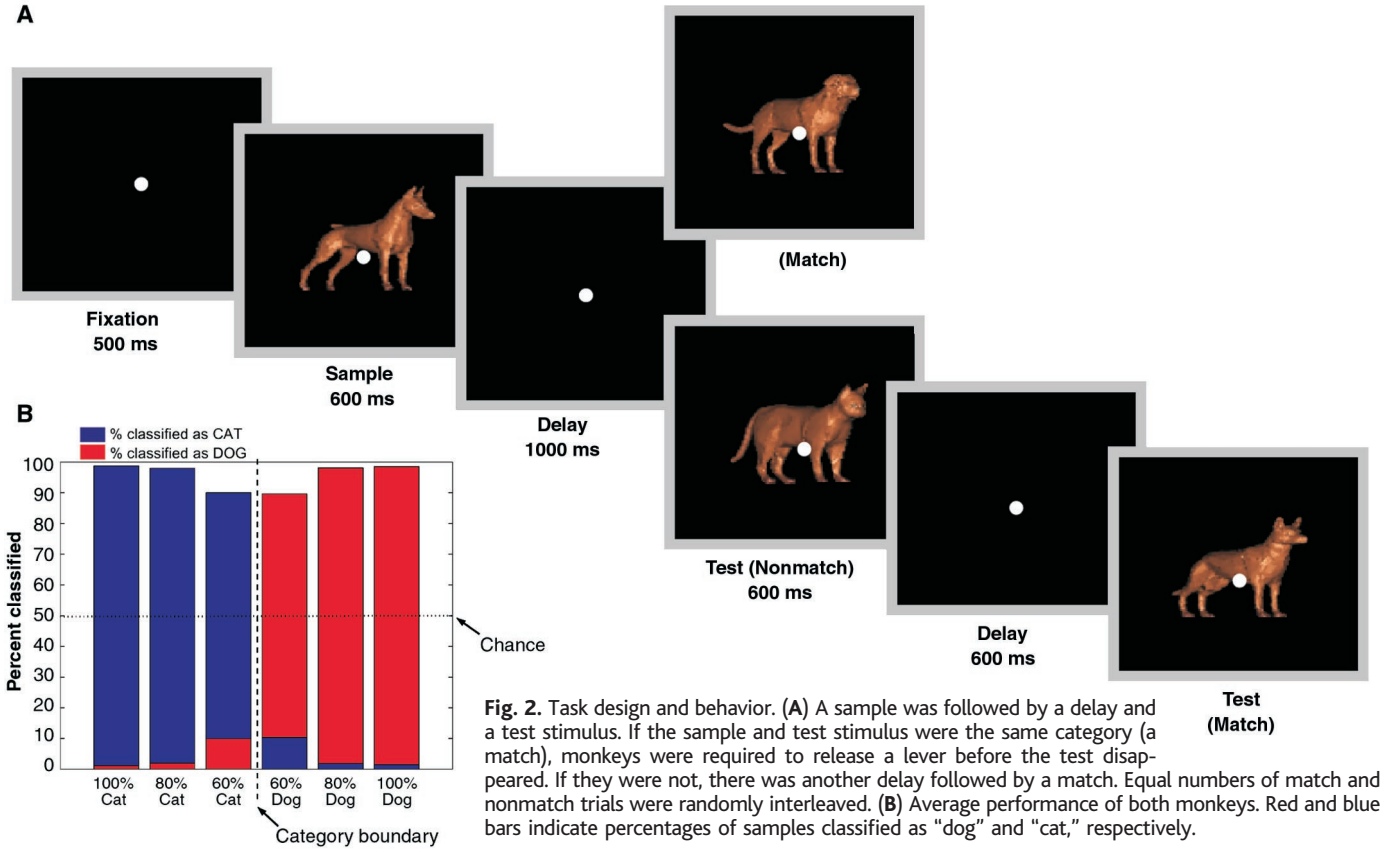

Fig. 2. Task design and behavior. (**A**) A sample was followed by a delay and a test stimulus. If the sample and test stimulus were the same category (a match), monkeys were required to release a lever before the test disappeared. If they were not, there was another delay followed by a match. Equal numbers of match and nonmatch trials were randomly interleaved. (**B**) Average performance of both monkeys. Red and blue bars indicate percentages of samples classified as "dog" and "cat," respectively.

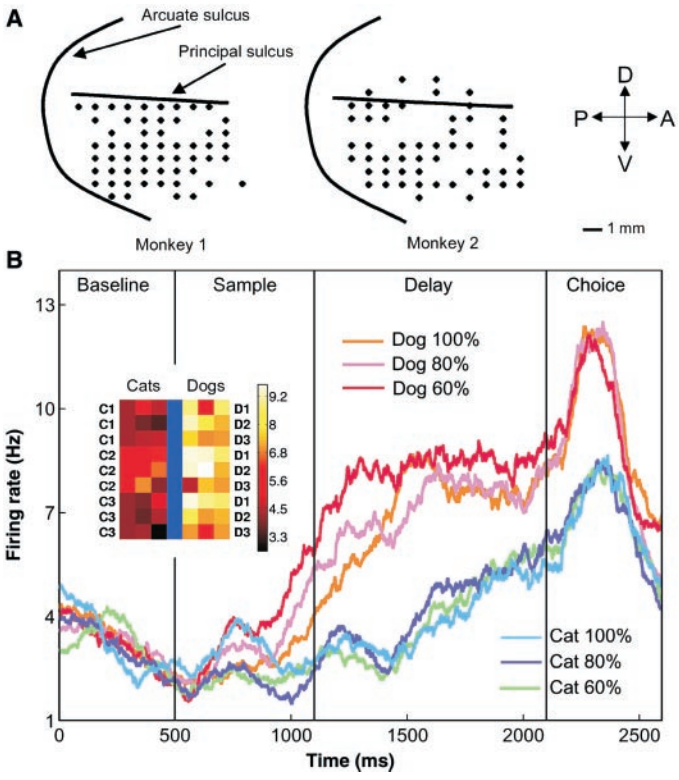

Fig. 3. Recording locations and single neuron example. (**A**) Recording locations in both monkeys. A, anterior; P, posterior; D, dorsal; V, ventral. There was no obvious topography to task-related neurons. (**B**) The average activity of a single neuron in response to stimuli at the six morph blends. The vertical lines correspond (from left to right) to sample onset, offset, and test stimulus onset. The inset shows the neuron's delay activity in response to stimuli along each of the nine between-class morph lines (see Fig. 1). The prototypes (C1, C2, C3, D1, D2, and D3) are represented in the outermost columns; each appears in three morph lines. A color scale indicates the activity level.

in activity during the sample and/or the delay interval to cats versus dogs. Similar numbers of neurons preferred cats (sample interval, 35/65; delay interval, 21/44) and dogs (sample, 30/65; delay, 23/44).

Figure 3B shows an example of a single neuron that exhibited greater activity in response to dogs than to cats and responded similarly to samples from the same category, regardless of their degree of dogness or catness. Its activity was different in response to stimuli near the category boundary, the cat-like dogs (60:40 dog:cat) versus the dog-like cats (60:40 cat:dog) (*22*), but there was no difference in activity elicited by these stimuli and by their respective prototypes (the 100% cats or dogs) (*23*). The inset in Fig. 3B shows the neuron's activity in response to each of the 54 samples. It exhibited overall greater activity in response to dogs than to cats, but there were small differences within categories. Just a few stimuli elicited activity that was similar to that from the other category. These stimuli were not consistent across different neurons, however. Across the population of neurons, category activity appeared at the start of neural responses to the sample, about 100 ms after sample onset (*24*).

We examined all stimulus-selective neurons, irrespective of whether they were category-selective per se (*25*). For each neuron, we computed the difference in activity between pairs of samples at different positions along each between-category morph line (Fig. 1A). In Fig. 4, A and B, each neuron's average difference in response to pairs of samples from the same category (within-category difference, WCD) is plotted against its difference in response to samples from different categories (between-category difference, BCD). If neurons were not sensi-

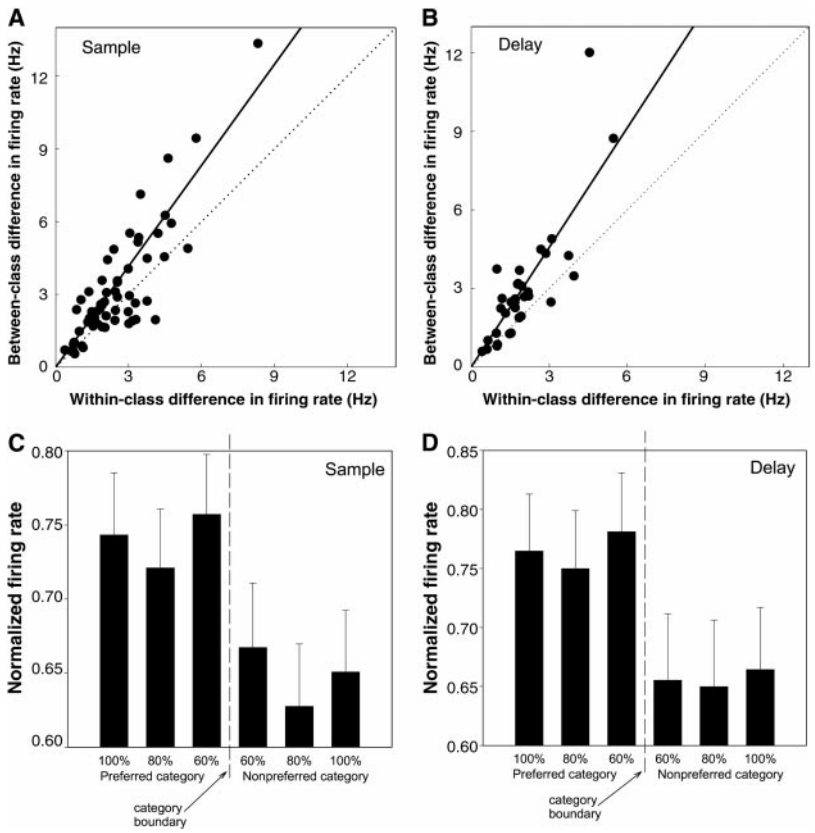

Fig. 4. Category effects in a neural population. (**A** and **B**) Average differences in activity in response to samples from the same (WCD) and different (BCD) categories for the sample (A) and delay interval (B). Each point represents one neuron. The dotted line indicates equal differences irrespective of category. The solid line indicates the regression line. (**C** and **D**) Average activity of the neural population (and standard error) in response to stimuli at different morph levels of their preferred and nonpreferred categories for the sample (C) and delay (D) intervals.

tive to categories, these measures should be similar (i.e., BCD/WCD ratios should equal 1 and cluster around the diagonal). Instead, the BCD values are significantly higher than WCD values. This indicates greater activity differences in response to samples from different categories, especially during the delay (*26*).

The average activity of all stimulus-selective neurons at different morph levels is shown in Fig. 4, C and D (*27*). There was a significant difference in activity between the categories (*28*), but activity was similar at the different morph levels within each category (*29*), indicating greater sensitivity to stimulus category than to identity. Few category-selective neurons conveyed significant identity information (sample interval, 20/65 or 31%; delay interval, 10/44 or 23%) (*30*). Also, PF neural responses to the test stimulus seemed to reflect category evaluation. Many PF neurons showed enhanced or suppressed activity when the test stimulus matched the category of the sample (112/395 or 28%) (*31*). Similar effects were reported for identity matches in the PF and IT cortex (*32*).

Because our monkeys had no experience with cats or dogs before training, it seemed likely that the categories were learned. We thus retrained one monkey on the DMC task after defining two new category boundaries that were orthogonal to the original boundary (Fig. 1A). This created three new classes, each containing morphs centered around one cat prototype and one dog prototype (e.g., the cheetah and the "doberman"). After training, the monkey was able to perform the new three-category DMC task at >85% correct. We then recorded from 103 PF neurons from the same depths and locations in the PF cortex, using the same samples as in the original two-category task.

Neural responsiveness (58% or 60/103) (*33*) and stimulus-selectivity (35% or 21/60) (*34*) during the three-category task was similar to that during the two-category task (64% or 253/395, and 28% or 73/253, respectively), but the original categories were no longer reflected in activity (*35*). Instead, the three new categories were evident in delay activity (*36*). As during the two-category task, category information was stronger during the delay (*37*), possibly because it is relevant for the judgment after the delay. "Prospective activity" is stronger nearer the relevant event (*38, 39*) and appears earlier within a trial as task proficiency increases (*40*). The monkey was not as proficient at the three-category task, and its reaction times were significantly longer (*41*).

Categorization of sensory inputs is the nexus between perception and cognition; thoughts and behaviors depend on knowledge of the types of things around us. The sharp transition in neural activity we observed is consistent with a "classical," perceptual category boundary. More conceptual categories can have "fuzzy" boundaries and are unlikely to exhibit such properties (*42*). Perceptual categorization relies on extraction of the combinations of features defining a category. These features were not explicitly instructed, were acquired by training, and were necessarily multivariate abstractions; the categories differed by more than a few simple features. PF activity could have reflected, and/or resulted in, a shifting of attention to those features (*43*).

These results fit well with studies suggesting that PF neural circuitry is malleable. Experience has been shown to induce and modify the sensitivity of PF neurons to specific stimuli (*44, 45*), and PF activity reflects learned associations and rules (*40, 46, 47*). Of course, the PF cortex is not likely to be the only brain area involved in categorization. The PF cortex is interconnected with temporal lobe structures important for long-term memory (*48*), including the IT cortex, whose neurons have stimulus specificities that could contribute to categorization (*7, 49*). Interactions between the PF and IT cortices underlie the storage and/or recall of visual memories and associations (*50–52*), but not necessarily visual short-term memory (*53*). The storage and recall of categories may also require such collaboration.

References and Notes

1. L. W. Barsalou, *Cognitive Psychology: An Overview for Cognitive Scientists* (Erlbaum, Hillsdale, NJ, 1992).
2. W. A. Roberts, D. S. Mazmanian, *J. Exp. Psychol. Anim. Behav. Proc.* **14**, 247 (1988).
3. M. Fabre-Thorpe, G. Richard, S. J. Thorpe, *Neuroreport* **9**, 303 (1998).
4. R. Vogels, *Eur. J. Neurosci.* **11**, 1223 (1999).
5. T. Orlov, V. Yakovlev, S. Hochstein, E. Zohary, *Nature* **404**, 77 (2000).
6. R. Desimone, T. D. Albright, C. G. Gross, C. Bruce, *J. Neurosci.* **4**, 2051 (1984).
7. E. Kobatake, K. Tanaka, *J. Neurophysiol.* **71**, 856 (1994).
8. N. K. Logothetis, J. Pauls, T. Poggio, *Curr. Biol.* **5**, 552 (1995).
9. D. I. Perrett, J. K. Hietanen, M. W. Oram, P. J. Benson, *Philos. Trans. R. Soc. London Ser. B* **335**, 23 (1992).
10. C. G. Gross, in *Handbook of Sensory Physiology*, R. Jung, Ed. (Springer-Verlag, Berlin, 1973), pp. 451–482.
11. K. Tanaka, *Annu. Rev. Neurosci.* **19**, 109 (1996).
12. E. K. Miller, *Nature Rev. Neurosci.* **1**, 59 (2000).
13. R. A. Wyttenbach, M. L. May, R. R. Hoy, *Science* **273**, 1542 (1996).
14. D. Beymer, T. Poggio, *Science* **272**, 1905 (1996).
15. C. Shelton, *Int. J. Comput. Vision* **38**, 75 (2000).
16. We used an algorithm that found corresponding points between one of the prototypes and the others and computed their differences as vectors. Morphs were linear combinations of these vectors added to the prototype (for more information, see www.ai.mit.edu/people/cshelton/corr). The cat and dog stimuli differed along multiple features and were smoothly morphed (i.e., without sudden appearance of any feature). Images were 4.2° in diameter, had identical color, shading, orientation, and scale, and were presented at the center of gaze.

17. For neurophysiological recording, morphs were six levels of blends of cat and dog (100:0, 80:20, 60:40, 40:60, 20:80, 0:100) and two levels within categories (60:40, 40:60).
18. "Similarity" as defined by the morphing technique and confirmed by an image correlation analysis.
19. Monkeys maintained gaze within 2° of a fixation point throughout the trial. Eye movements were monitored using an eye tracking system (ISCAN, Cambridge, MA). We excluded stimuli that were less than 60% of a given category, as they carried little or no category information. To prevent memorization of sample-test pairs, we chose as the test stimuli a set of 200 randomly generated morphs that were at least 70% of a category. All main effects were observed in both monkeys. For brevity, we summarize their data.
20. This total consisted of 130 neurons from one monkey and 265 from the other. Sample interval activity was summed over 800 ms, beginning 100 ms after stimulus onset. The delay interval activity was summed from 300 ms after sample offset to 100 ms after the end of the delay. Baseline activity was from the 500 ms of fixation before sample onset.
21. *T* test versus baseline activity, $P < 0.01$. Parametric statistics such as *t* tests assume normal distributions. Because neuronal activity is sometimes not normally distributed, we also computed nonparametric statistics for all main effects. They yielded a virtually identical pattern of results.
22. *T* tests on activity from the sample and delay intervals, both $P < 0.001$.
23. $P > 0.6$.
24. Paired *t* tests between activity of all stimulus-selective neurons in response to the two categories computed in successive 100-ms time bins. A significant difference ($P < 0.01$) began 100 to 200 ms after sample onset, when the earliest PF neurons began responding. The immediate appearance of category information was also evident in average histograms across the neuron population.
25. One-way analysis of variance (ANOVA) on the 54 sample stimuli. Sample interval, 62 neurons; delay interval, 33 neurons; $P < 0.01$.
26. *T* test that BCD/WCD ratios were significantly different from 1. Sample interval, BCD/WCD mean = 1.30; delay interval, BCD/WCD mean = 1.49; both $P < 0.001$. Category information was significantly stronger during the delay; one-tailed *t* test, $P = 0.04$. An index of (BCD − WCD)/(BCD + WCD) yielded similar results.
27. Excluding neurons with firing rates below 2 Hz (which produce spurious values when normalized) yielded 55 and 29 neurons with selectivity in the sample and delay intervals, respectively. We normalized each neuron's activity as a proportion of its activity in response to the most effective morph level. To ensure that analyses were not biased toward a category effect, we used only the single stimulus that evoked the maximum response to determine preferred and nonpreferred category.
28. Two-way ANOVA of category membership and level of category (60%, 80%, 100%), test of the category factor. $P < 0.01$ for both intervals.
29. Two-way ANOVA, test of the level factor, $P > 0.6$ for both intervals.
30. ANOVAs on the 27 samples from the preferred or nonpreferred category, either $P < 0.01$.
31. *T* test on all match versus all nonmatch test stimuli, $P < 0.01$.
32. E. K. Miller, C. A. Erickson, R. Desimone, *J. Neurosci.* **16**, 5154 (1996).
33. *T* test versus baseline for the sample and/or delay intervals, $P < 0.01$.
34. One-way ANOVA on all 54 samples for the sample and/or delay intervals, $P < 0.01$.
35. Sample interval, mean two-category BCD/WCD = 1.13, *t* test, $P = 0.22$; delay interval, two-category BCD/WCD mean = 0.96, *t* test, $P = 0.58$. This analysis was limited to morphs between corresponding cat and dog prototypes (i.e., C1-D1, C2-D2, C3-D3; the vertical morph lines in Fig. 1A) because the other morph lines crossed both the two-category and three-category boundaries. We confirmed that this test could detect two-category information by applying it to the data from the two-category task. The results were virtually identical to the two-category test described above (sample interval, BCD/WCD ratio = 1.33, *t* test, $P < 0.001$; delay interval, BCD/WCD ratio = 1.57, *t* test, $P < 0.001$).
36. Three-category BCD/WCD mean = 1.51, *t* test, $P < 0.01$. As for the two-category test, we compared samples at equivalent distances along between-category morph lines but now using morph lines that crossed the three-category boundaries, but not the two-category boundary. The early appearance of category information in PF activity also suggested that training had altered neuronal selectivity.
37. It was not evident during the sample interval; three-category BCD/WCD mean = 1.03, *t* test, $P = 0.79$.
38. J. Quintana, J. M. Fuster, *Neuroreport* **3**, 721 (1992).
39. G. Rainer, S. C. Rao, E. K. Miller, *J. Neurosci.* **19**, 5493 (1999).
40. W. F. Asaad, G. Rainer, E. K. Miller, *Neuron* **21**, 1399 (1998).
41. Performance was lower on the three-category task than on the two-category task (87% versus 96%, *t* test, $P < 0.001$) and reaction times were longer (average 307 ms versus 264 ms, *t* test, $P < 0.001$).
42. G. Lakoff, *Women, Fire, and Dangerous Things* (Univ. of Chicago Press, Chicago, 1987).
43. R. Dias, T. W. Robbins, A. C. Roberts, *Nature* **380**, 69 (1996).
44. N. P. Bichot, J. D. Schall, K. G. Thompson, *Nature* **381**, 697 (1996).
45. G. Rainer, E. K. Miller, *Neuron* **27**, 179 (2000).
46. I. M. White, S. P. Wise, *Exp. Brain Res.* **126**, 315 (1999).
47. W. F. Asaad, G. Rainer, E. K. Miller, *J. Neurophysiol.* **84**, 451 (2000).
48. M. J. Webster, J. Bachevalier, L. G. Ungerleider, *Cereb. Cortex* **4**, 470 (1994).
49. R. Vogels, *Eur. J. Neurosci.* **11**, 1239 (1999).
50. S. A. Gutnikov, Y. Y. Ma, D. Gaffan, *Eur. J. Neurosci.* **9**, 1524 (1997).
51. G. Rainer, S. C. Rao, E. K. Miller, *J. Neurosci.* **19**, 5493 (1999).
52. H. Tomita, M. Ohbayashi, K. Nakahara, I. Hasegawa, Y. Miyashita, *Nature* **401**, 699 (1999).
53. D. Gaffan, M. J. Eacott, *Exp. Brain. Res.* **105**, 175 (1995).
54. We thank C. Shelton for the morphing software, and K. Anderson, W. Asaad, M. Histed, M. Mehta, J. Wallis, R. Wehby, and M. Wicherski for valuable comments, help, and discussions. Supported by a National Institute of Neurological Disorders and Stroke grant, a NSF Knowledge and Distributed Intelligence grant, the RIKEN-MIT Neuroscience Research Center, a Merck/MIT Fellowship (M.R.), the Whitaker Chair (T.P.), and the Class of 1956 Chair (E.K.M.).

1 September 2000; accepted 15 November 2000

Role of ER Export Signals in Controlling Surface Potassium Channel Numbers

Dzwokai Ma,[1] Noa Zerangue,[1] Yu-Fung Lin,[1] Anthony Collins,[2] Mei Yu,[1] Yuh Nung Jan,[1] Lily Yeh Jan[1]*

Little is known about the identity of endoplasmic reticulum (ER) export signals and how they are used to regulate the number of proteins on the cell surface. Here, we describe two ER export signals that profoundly altered the steady-state distribution of potassium channels and were required for channel localization to the plasma membrane. When transferred to other potassium channels or a G protein–coupled receptor, these ER export signals increased the number of functional proteins on the cell surface. Thus, ER export of membrane proteins is not necessarily limited by folding or assembly, but may be under the control of specific export signals.

Ion channels control neuronal signaling, hormone secretion, cell volume, and salt and water flow across epithelia (*1*). The number of cell surface channels is critical to these physiological functions (*1*). Whether forward-trafficking signals regulate the supply of ion channels to the plasma membrane is not known.

Export from the ER to the Golgi is a key early event in forward traffic. Numerous studies suggest that ER export is limited primarily by quality control (*2, 3*). However, certain secreted and membrane proteins are concentrated in the process of ER export (*4–6*). A motif containing Asp, a variable amino acid, and Glu (DXE) (*7–9*) in vesicular stomatitis virus glycoprotein (VSV-G) has been reported to accelerate the ER export. It is not clear whether ER export signals control the steady-state levels of endogenous membrane proteins destined for later compartments, including the plasma membrane.

The inwardly rectifying potassium (Kir) channels (*10*) Kir1.1 (ROMK1) and Kir2.1 (IRK1) were efficiently expressed in the plasma membrane in *Xenopus* oocytes, whereas several other Kir family members exhibited poor expression or delayed expression kinetics. To test whether these differences correlate with the presence or absence of trafficking signals, we first examined the possible involvement of the variable COOH-termini of these channels (Fig. 1A). Indeed, efficient surface expression (*11*)

[1]Howard Hughes Medical Institute, University of California, San Francisco, San Francisco, CA 94143–0725, USA. [2]College of Pharmacy, Oregon State University, Corvallis, OR 97331–3507, USA

*To whom correspondence should be addressed. E-mail: gkw@itsa.ucsf.edu